A LTI/LQE SCHEME FOR REAL TIME ROTOR COMPONENT LOAD ESTIMATION

J.V.R Prasad
Jvr.prasad@ae.gatech.edu

Chams E. Mballo
Cmballo3@gatech.edu

School of Aerospace Engineering
Georgia Institute of Technology
Atlanta, GA 30332, USA

Abstract

Accurate and real-time load monitoring of vital components located in the rotor system is important not only for inferring usage and estimating fatigue in those components but also for developing load alleviation control schemes. An approach for on-line estimation of rotor component loads is presented in this paper in which a linear time invariant (LTI) model of helicopter coupled body/rotor dynamics is combined with a Linear Quadratic Estimator (LQE), which is designed to correct LTI model state response using fixed system measurements. The developed LTI/LQE scheme is evaluated in simulation using a nonlinear model of a generic helicopter for on-line prediction of rotor blade pitch link loads arising from vehicle maneuvers.

1. NOMENCLATURE

A	LTI state matrix
B	LTI input matrix
C	LTI output matrix
D	LTI direct transmission matrix
E	Harmonic reconstruction matrix
L	Discrete time LTI state matrix
Fx, Fy, Fz	Fixed system rotor hub forces
$F(\psi)$	LTP state matrix
$G(\psi)$	LTP input matrix
K	Kalman gain matrix
Mx, My, Mz	Fixed system rotor hub moments
N	Discrete time LTI output matrix
P	Filter error covariance
$P(\psi)$	LTP output matrix
P, Q, R	Body roll, pitch and yaw rates (Figs. 5 and 9)
Q	Process noise covariance matrix
R	Measurement Noise covariance Matrix
$\mathrm{R}(\psi)$	LTP direct transmission matrix
U	Augmented control vector
U, V, W	Vehicle body axes velocity components (Figs. 6 and 10)
X	Augmented state vector
Y	Augmented output vector
s	Measurement estimate
u	Control vector
v	Measurement noise
w	Process noise
x	State vector
y	Output vector
z	Measurement
ψ	Non-dimensional time
$()_0$	Average or zeroth harmonic term
$()_{nc}$	n^{th} cosine harmonic term
$()_{ns}$	n^{th} sine harmonic term
$()_k$	k^{th} iteration
$()_x$	Longitudinal axis
$()_y$	Lateral axis
$()_z$	Vertical axis
$()_-$	Previous Iteration

2. INTRODUCTION

A 2012 survey of the past 30 years, carried out within Augusta Westland Limited (AWL) Materials Technology Laboratory, concluded that fatigue failures account for approximately 55% of all premature failures in helicopter components[1]. The causes of low cycle fatigue are largely due to aircraft maneuvers, gust loading and through takeoff and landing. Critical helicopter components, classified as Grade-A Vital components by regulatory authorities, are subject to significant fatigue loading in which the failure would result in a catastrophic event. A list of fatigue critical components[2] on the AH-64A Apache shows that many of the Grade-A Vital components are located in the rotor system, creating challenges for real time load monitoring of those components.

Current methods for structural health and usage monitoring and load alleviation control rely on distributed sensing and operational monitoring to infer usage and estimate fatigue in critical components. Such inference process is affected by significant uncertainty given that sensors' type and locations are often removed from hot spot areas characterized by maximum stresses. For example, past work[3] for limiting pitch link loads used proxy models of the vibratory loading. A classic example is the Equivalent Retreating Indicated Tip Speed (ERITS) parameter, which has been correlated as a function of airspeed and normal load factor with vibratory pitch link loads from retreating blade stall onset, can be limited to indirectly constrain the pitch link loads.

A recent Penn State study[4] (see Figure 1 taken from Ref. 4) used curve fits of pitch link vibratory loads as function of aircraft states and demonstrated the potential for limiting the peak-to-peak pitch link loads by limiting roll rate in a high fidelity FLIGHTLAB® simulation of a utility helicopter, thereby reducing incremental fatigue damage (as measured by a crack growth model), in this case, by over 50% (shown as 'DMC' in Figure 1) for a roll reversal maneuver. The role rate limiting resulted in no degradation in handling qualities when evaluated using the ADS-33 attitude quickness and bandwidth specifications.

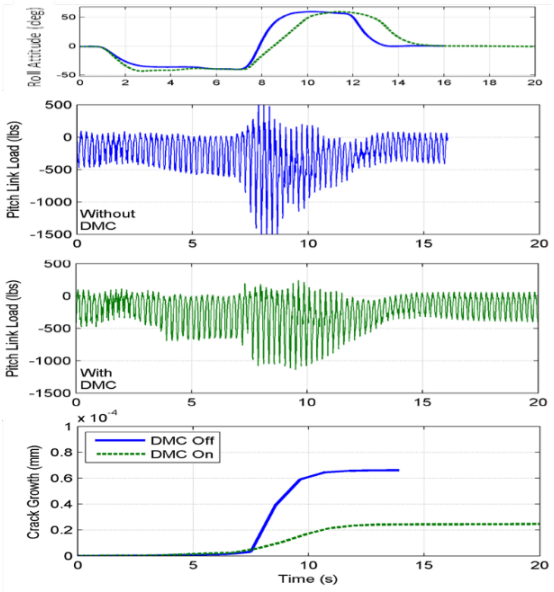

Figure 1. Reduction of vibratory pitch link load using roll rate limiting technique. (Ref. 4)

Recent work[5,6] at Georgia Tech has developed methods for approximation of coupled body/rotor dynamics using high order Linear Time Invariant (LTI) models. These methods use harmonic decomposition to represent higher frequency harmonics as states in an LTI state space model, and they offer the potential for real-time estimation of the effect of control inputs on component dynamic loads, which in turn can be used in combination with reduced order structural models to estimate primary damage variables associated with fatigue of critical components. Such real-time estimation of component level dynamic loads, stresses and strains, etc., provides the opportunity for real-time monitoring of component damage variables, and the

development of control schemes designed to alleviate component fatigue damage.

The present study is focused on developing a real time algorithm for estimation of component level dynamic loads arising from vehicle maneuvers. It explores on-line use of LTI models of coupled body/rotor dynamics, a Linear Quadratic Estimator (LQE), and fixed system measurements for estimation of rotating system component loads.

3. LTI/LQE MODEL

A detailed description of the proposed LTI/LQE scheme for component load estimation is presented in this section. Considering an LTP model of the form given in Eqs. (1) and (2), harmonic decomposition for an extraction of LTI model assumes the approximation for the state vector, x, in Eq. (3)

(1) $$\dot{x} = F(\psi)x + G(\psi)u$$

(2) $$y = P(\psi)x + R(\psi)u$$

(3) $$x = x_0 + \sum_{n=1}^{N} x_{nc}\cos n\psi + x_{ns}\sin n\psi$$

where x_0 is the average component and x_{nc} and x_{ns} are respectively the n/rev cosine and sine harmonic components of x. Likewise, the control u is expanded in terms of harmonic components as

(4) $$u = u_0 + \sum_{m=1}^{M} u_{mc}\cos m\psi + u_{ms}\sin m\psi$$

and the output y is expanded in terms of harmonic components as

(5) $$y = y_0 + \sum_{l=1}^{L} y_{lc}\cos l\psi + y_{ls}\sin l\psi$$

where y_o is the average component and y_{lc} and y_{ls} are respectively the l^{th} harmonic cosine and sine components of y.

The LTI approximation of the LTP model given by Eqs. (1) and (2) can be obtained by substituting for harmonic expansions of x, u and y, i.e., Eqs. (3), (4), and (5) into Eqs. (1) and (2) (see Refs. 5 and 6 for details). The resulting equations can be represented in state-space matrix form by defining an augmented state vector as:

(6) $$X = \left[x_0{}^T .. x_{ic}{}^T\ x_{is}{}^T .. x_{jc}{}^T\ x_{js}{}^T ..\right]^T$$

and the augmented control vector as

(7) $$U = [u_0{}^T .. u_{mc}{}^T\ u_{ms}{}^T ....]^T$$

where x_0 is the zeroth harmonic component, x_{ic}, x_{is} are the i^{th} harmonic cosine and sine components of x, and u_0 is the zeroth harmonic and u_{mc}, u_{ms} are the m^{th} harmonic cosine and sine components of u, respectively. The state equation of the resulting LTI model is

(8) $$\dot{X} = [A]X + [B]U$$

Likewise, the augmented output vector of the LTI model is defined as

(9) $$Y = [y_0{}^T .. y_{lc}{}^T\ y_{ls}{}^T ....]^T$$

Then the output equation of the LTI model can be written as

(10) $$Y = [C]X + [D]U$$

Detailed expressions for the LTI model matrices A, B, C and D are developed in Ref. 6.

In order for construction of an LTI/LQE model[7], the LTI model of Eqs. (8) and (10) are represented in discrete form including process and measurement noise terms as Eqs. (11) and (12)

(11) $$X_k = [L]X_{k-1} + [N]U_{k-1} + w_{k-1}$$

(12) $$Y_k = [C]X_k + [D]U_k + v_k$$

where the random variables, w and v, represent the process and measurement noise, respectively. They are assumed to be

independent, zero-mean white noise with normal probability distributions given by Eqs. (13) and (14)

(13) $$p(w) \sim N(0, Q)$$

(14) $$p(v) \sim N(0, R)$$

where Q and R are the process noise covariance and measurement noise covariance matrices, respectively.

The goal of the LQE (Kalman filter) is to compute *a posteriori* state estimate, $\hat{X}_k$, as a linear combination of an *a priori* estimate, $\hat{X}_k^-$, and the weighted difference between an actual measurement, z_k, and a measurement prediction, s_k, as shown in Eq. (15).

(15) $$\hat{X}_k = \hat{X}_k^- + K_k(z_k - s_k)$$

The difference $(z_k - s_k)$ is called the measurement innovation, or the residual, and K is referred to as the Kalman gain matrix that minimizes the *a posteriori* error covariance.

The Kalman filter algorithm estimates a process by predicting future response using the previous state estimate, current control input, and the system model, then corrects that prediction using current measurement data. As such, the equations for the Kalman filter fall into two groups: time update equations and measurement update equations. The time update equations first project the system state and error covariance estimates forward in time using the current control vector to predict the future states and error covariance given the estimate from the previous time step and the system model. These equations are presented as Eqs. (16) and (17)[8].

(16) $$\hat{X}_k^- = L\hat{X}_{k-1} + NU_{k-1}$$

(17) $$P_k^- = FP_{k-1}F^T + Q$$

The measurement update equations generate an improved *a posteriori* estimate by correcting the *a priori* estimate with current measurement data weighted against the *a priori* estimate using the estimated error covariance.

(18) $$K_k = P_k^- C^T (CP_k^- C^T + R)^{-1}$$

(19) $$\hat{X}_k = \hat{X}_k^- + K_k(z_k - s_k)$$

(20) $$P_k = (I - K_k C)P_k^-$$

Since the objective of the proposed LTI/LQE scheme is to correct the LTI model state response using fixed system measurements, and, in turn, use the corrected LTI state response for the estimation of rotating system component loads, we consider, in this study, the total hub loads as the measurement, z. Since the total hub loads can be obtained as a linear combination of the LTI outputs, the measurement equation used to determine s is defined as follows:

(21) $$s_k = E(\psi)\hat{Y}_k^- = E(\psi)C\hat{X}_k^- + E(\psi)DU_{k-1}$$

(22) $$E(\psi) = [I \quad I\cos i\Omega t \quad I\sin i\Omega t \quad \cdots \quad I\cos j\Omega t \quad I\sin j\Omega t \quad \cdots]$$

where $E(\psi)$ is the time-periodic linear combination of LTI system outputs which comprises the total hub loads in the fixed frame. The measurement update equations are thus updated to reflect this augmented output as follows.

(23) $$K_k = P_k^- C^T E(\psi)^T (E(\psi)CP_k^- C^T E(\psi)^T + R)^{-1}$$

(24) $$P_k = (I - K_k E(\psi)C)P_k^-$$

With all system matrices and noise covariance matrices are constant or time periodic, the steady state solution to the Kalman gain matrix, K of Eq. (23), is periodic. Since calculation of the periodic steady state Kalman gain matrix does not depend on system state or time, it may be pre-calculated off-line for a given set of output and noise covariance matrices to improve the computation time associated with application of the LTI/LQE scheme. Thus, Eqs. (17), (23) and (24), can

be iteratively solved *a priori* for selected values of the process noise covariance (Q) and the measurement noise covariance (R) in Eqs. (13) and (14). A block diagram representation of the proposed LTI/LQE scheme for rotor component load estimation using fixed-system measurements is illustrated in Fig. 2.

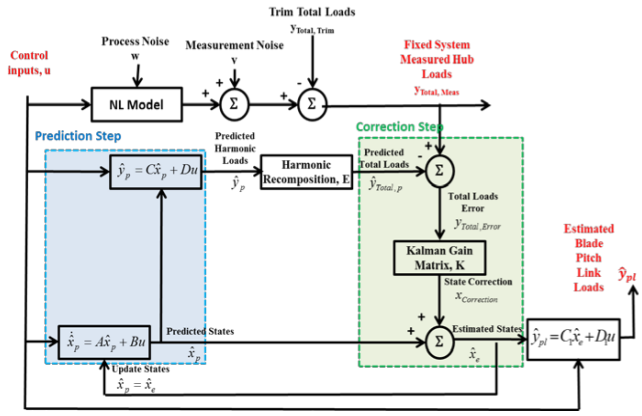

Figure 2. Block diagram of the proposed LTI/LQE scheme for rotor component load estimation.

4. RESULTS

The proposed LTI/LQE scheme was evaluated in simulation for the case of on-line estimation of blade pitch link loads arising from vehicle maneuvers using a nonlinear model of a generic helicopter in FLIGHTLAB®. Using the scheme for LTI model extraction from a nonlinear model presented in Ref. 6, an LTI model with harmonic decomposition of LTP states in a first order representation (i.e., separate displacement and velocity states) was developed from a full vehicle nonlinear (NL) FLIGHTLAB® model of a generic helicopter with elastic blade mode shapes and a 33-state Peters-He dynamic inflow model. The extracted LTI model has previously been validated through comparisons with the nonlinear model both in time and frequency domains and is found to be of sufficient fidelity[6]. The LTP model, developed from the NL model prior to being decomposed into harmonic states for the LTI system, included 8 body states, 33 inflow states (Peters-He Finite state inflow with 4 harmonics and a maximum radial variation power of 8), and 48 multi-blade coordinate (MBC) rotor states including elastic modes. Thus, the total number of LTP states is 89. Each of these LTP states was then decomposed into 0-8/rev harmonic components, resulting in 1513 total LTI model states. It should be noted that all 0-8 harmonics may not be required to achieve acceptable fidelity in the LTI model as discussed in Ref. 6. Future work should consider reduced order LTI models for reduced computational cost. The nonlinear model was trimmed at 120 knots. Figure 3 is a plot of the reference blade pitch link axial load variation with time at equilibrium from the nonlinear model.

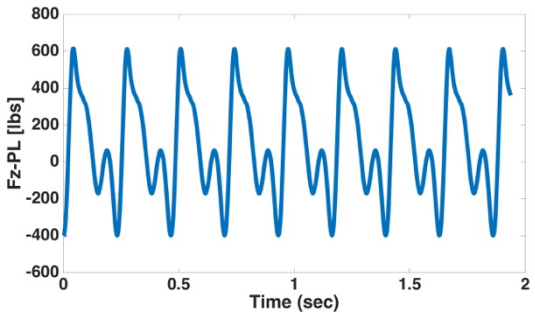

Figure 3. Steady state reference blade pitch link axial load variation with time.

4.1 Pitch maneuver (less aggressive)

To assess the performance of the LTI model, a less aggressive pitch maneuver was created using a combination of ramps in the longitudinal cyclic control.

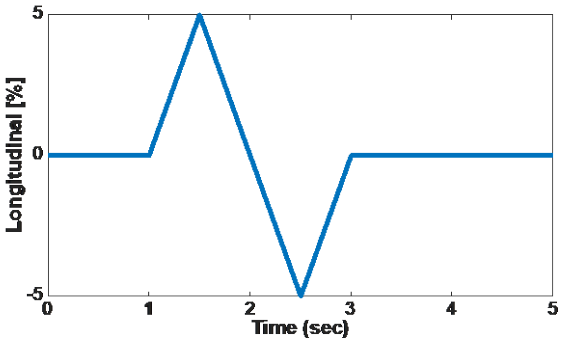

Figure 4. Percentage change from trim of longitudinal cyclic control input.

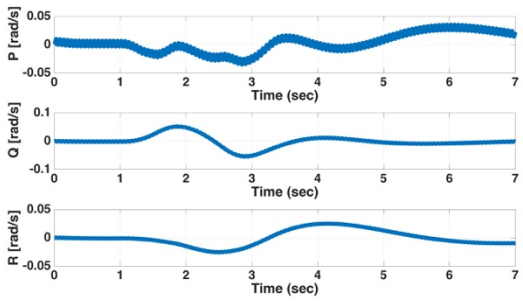

Figure 5. Body angular rate response from the nonlinear model for the selected longitudinal control input shown in Fig. 4.

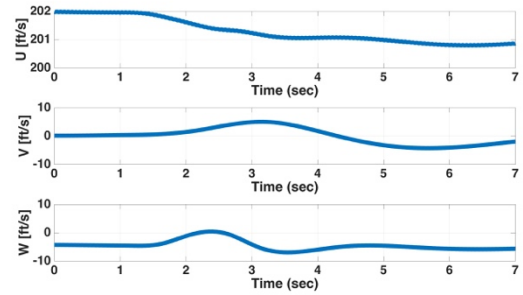

Figure 6. Body velocity response from the nonlinear model for the selected longitudinal control input shown in Fig. 4.

Figure 4 is a plot of the percentage change in longitudinal cyclic control variation applied both to the nonlinear model and the LTI model. All other controls were held fixed at their trim values. The vehicle angular rate responses (P, Q, R) and the body velocity component responses (U, V, W) from the nonlinear model are presented in Figs, 5 and 6. The vehicle pitch rate (Q) response stays within 0.05 rad/sec for the selected longitudinal cyclic control input. Hence, this is considered as a less aggressive maneuver in this study.

The resulting variation of the reference blade pitch link axial load as predicted by the LTI model is compared with that from the nonlinear model in Fig. 7, where the sub-plot in Fig. 7 is a close-up view of the comparison over a selected time window. It is seen from the results in Fig. 7 that the LTI model prediction of the blade pitch link axial load variation arising from the selected less aggressive pitch maneuver is nearly same as that from the nonlinear model.

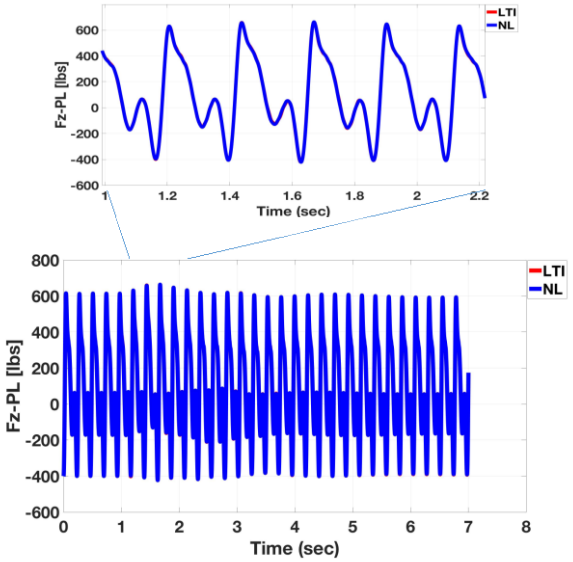

Figure 7. Axial pitch link load comparison between LTI and NL models for the selected longitudinal control input shown in Fig. 4.

4.2 Pitch maneuver (slightly more aggressive)

For further assessment of the fidelity of the LTI model for rotor blade pitch link load prediction, a slightly more aggressive pitch maneuver was simulated using the longitudinal cyclic control variation from trim shown in Fig. 9. Once again, all the other controls were held at their respective trim values.

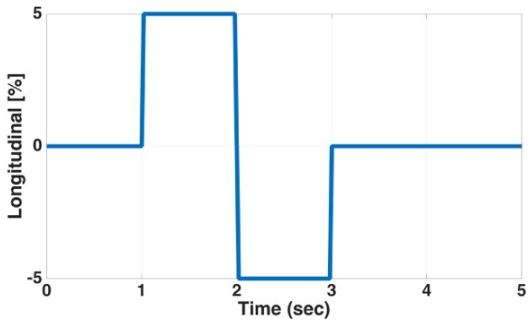

Figure 8. Percentage change from trim of longitudinal cyclic control input.

The resulting body angular rate and velocity responses from the nonlinear model simulation are shown in Figs. 10 and 11, respectively. The body pitch rate (Q) response goes up to 0.1 rad/sec for this case.

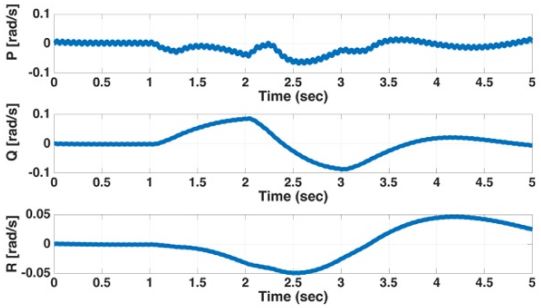

Figure 9. Body angular rate response from the nonlinear model for the selected longitudinal control input shown in Fig. 8.

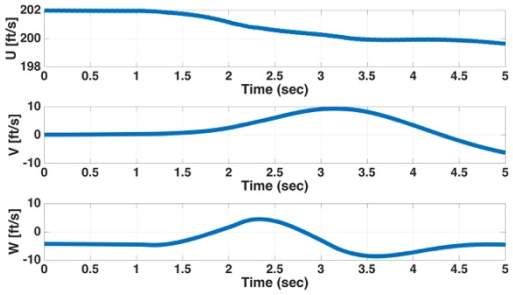

Figure 10. Body velocity response from the nonlinear model for the selected longitudinal control input shown in Fig. 8.

The reference blade pitch link axial load variation as predicted by the LTI model is compared with that of the nonlinear model in Fig. 11, with the inset figure showing a close-up view of the comparison over a selected time window. Now for this case of slightly more aggressive maneuver, differences between the LTI model predictions and the nonlinear model predictions of the blade pitch link loads are observed in Fig. 11. The observed differences are presumed to be associated with nonlinear effects becoming significant due to aggressiveness of the maneuver, which are not captured by the LTI model.

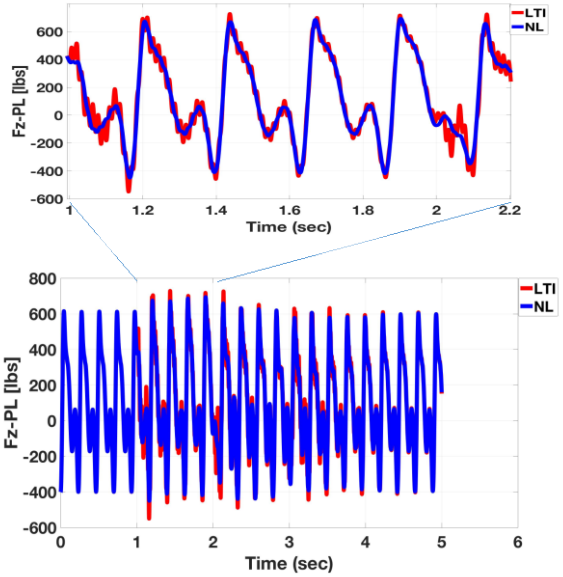

Figure 11. Axial pitch link load comparison between predictions from LTI and NL models for the selected longitudinal control input shown in Fig. 8.

4.3 LTI/LQE Performance

In order to improve the LTI model predictions for aggressive maneuvers, the LTI model is combined with a pre-designed Kalman filter using fixed system hub load response data from the nonlinear model as measurements to form the LTI/LQE scheme presented in Fig. 2. The form of the noise covariance matrices Q and R of Eqs. (13) and (14) for the Kalman filter design was selected to be diagonal as given in Eq. (25)

(25) $$Q = Q_0 * I \qquad R = R_0 * I$$

where I is the identity matrix, Q is a diagonal square matrix with size equal to the total number of states, and R is a diagonal square matrix with size equal to the total number of measurements. For this study, the values of Q_0 and R_0 in Eq. (25) were set to 10 and 10E-8, respectively. Since no explicit noise was added to the fixed system hub load response data, it was expected that the selected values of Q_0 and R_0 would allow the estimator to trust

the nonlinear hub load response much more than that of the LTI model response, and hence, correcting the LTI model response in order to make the LTI model predictions of the fixed system hub loads match with that of the nonlinear model. This aspect is verified by comparing the hub load predictions from the LTI and LTI/LQE with that of the nonlinear predictions for the slightly aggressive pitch maneuver case.

Figure 12 compares the fixed system hub loads (forces Fx, Fy and Fz and moments Mx, My and Mz) variations from trim as predicted by the LTI model with those of the nonlinear model for the slightly aggressive maneuver case. With the nonlinear model predictions representing the truth data, errors in LTI model predictions of hub loads can be seen in Fig. 12. The observed errors in LTI model predictions of hub loads are corrected by the proposed LTI/LQE scheme as seen from the results presented in Fig. 13, where estimates of hub load variations from trim from the LTI/LQE are compared with those from the nonlinear model. These observations are better illustrated in Fig. 14 where the differences between the LTI and the nonlinear model and the LTI/LQE and the nonlinear model of the hub loads predictions are compared. While the errors in LTI/LQE predictions stay near zero, LTI predictions show errors in Fig. 14.

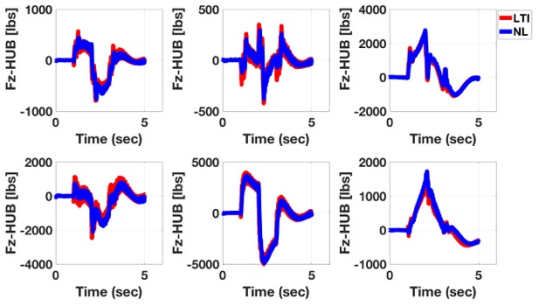

Figure 12. Comparison of fixed system hub load variations from trim between nonlinear (NL) model and LTI predictions.

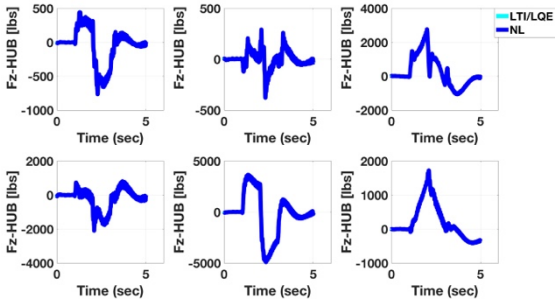

Figure 13. Comparison of fixed system hub load variations from trim between nonlinear model (NL) and LTI/LQE predictions.

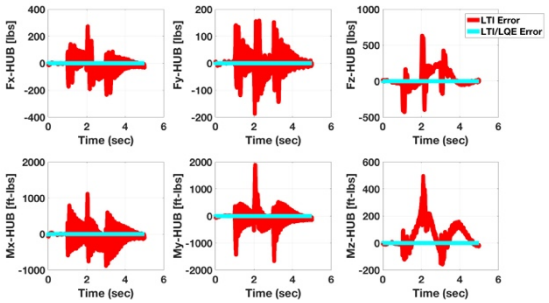

Figure 14. Comparison of error in fixed system hub load variations between LTI and LTI/LQE predictions.

From the results presented in Figs. 12 through 14, it is seen that LTI/LQE adjusts the LTI state responses in order to make its hub load predictions match with those of the nonlinear model. Hence, correction to the LTI model prediction of blade pitch link loads can be expected, provided, all, or at least the important, harmonic states of the LTI model are observable in the selected fixed system measurements. Figure 15 compares the error in blade pitch link load variation between LTI and LTI/LQE predictions. As expected, the LTI/LQE pitch link load predictions have less error when compared to that of the LTI model. While the LTI model predictions are improved by the LTI/LQE scheme, there are still significant errors seen during initial parts of the responses to control changes. This is felt to be due to non-observability of certain harmonic

components of the LTI model states in the fixed system hub load responses.

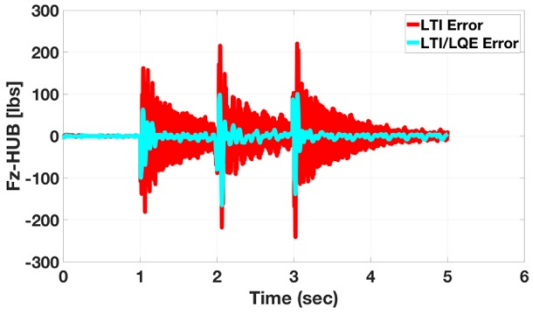

Figure 15. Comparison of error in reference blade axial pitch link load predictions between LTI and LTI/LQE.

5. CONCLUDING REMARKS

An approach for on-line estimation of rotor component loads is presented in which a linear time invariant (LTI) model of a helicopter coupled rotor/body dynamics is combined with a Kalman filter. The Kalman filter is designed to use fixed system measurements (for example, fixed system hub load measurements) in order to correct the LTI model state responses. The corrected LTI model state responses are in turn used for prediction of rotor system component loads.

The proposed LTI/LQE scheme is evaluated in simulation for on-line estimation of rotor blade pitch link loads arising from vehicle maneuvers using a nonlinear model of a generic helicopter in FLIGHTLAB®. The Kalman filter uses fixed system hub load responses from the nonlinear model as measurements. The presented results show promise in the ability of the proposed LTI/LQE scheme to improve LTI model predictions of blade pitch link loads for the maneuver considered in this study.

While the LTI model predictions are improved by the LTI/LQE scheme, there are still significant errors seen during initial parts of the responses to control changes. This is felt to be due to non-observability of certain harmonic states of the LTI model in the fixed system hub load responses used as measurements in this study. Future work needs to address this issue by using other fixed system measurements for LTI model state response corrections.

6. ACKNOWLEDGMENTS

This study is supported under the NRTC Vertical Lift Rotorcraft Center of Excellence (VLRCOE) from the U.S. Army Aviation and Missile Research, Development and Engineering Center (AMRDEC) under Technology Investment Agreement W911W6-17-2-0002, entitled Georgia Tech Vertical Lift Research Center of Excellence (GT-VLRCOE) with Dr. Mahendra Bhagwat as the Program Manager. The authors would like to acknowledge that this research and development was accomplished with the support and guidance of the NRTC. The views and conclusions contained in this document are those of the authors and should not be interpreted as representing the official policies, either expressed or implied, of the AMRDEC or the U.S. Government. The U.S. Government is authorized to reproduce and distribute reprints for Government purposes notwithstanding any copyright notation thereon.

7. REFERENCES

[1] Davies, D.P., Jenkins, S.L, and Belben, F.R., “Survey of fatigue failures in helicopter components and some lessons learnt,” Materials Technology Laboratory, Agusta Westland Limited, United Kingdom, 2012.

[2] Kaye, M., “Dynamic Health and Usage Monitoring System - Program Update,” Proceedings of the Fifteenth European Rotorcraft Forum, Amsterdam, Netherland, September 12-15, 1989.

[3] Jeram, G. and Prasad, J.V.R., “Open Architecture for Helicopter Tactile Cueing Systems,” Journal of the American Helicopter Society, Vol. 50, No. 3, July 2005, pp. 238-248.

[4] Caudle, D.B. “Damage Mitigation for Rotorcraft through Load Alleviating Control,” M.S. Thesis, The Pennsylvania State University, December 2014.

[5] Prasad, J. V. R., Olcer, F. E., Sankar, L. N. and He, C., “Linear Time Invariant Models for Integrated Flight and Rotor Control,” Proceedings of the 35th European Rotorcraft Forum, Hamburg, Germany, September 22 – 25, 2009

[6] Lopez, M. J. S. and Prasad, J. V. R., “Linear Time Invariant Approximations of Linear Time Periodic Systems,” Journal of the American Helicopter Society, Vol. 62, No. 1, Jan. 2017.

[7] Morgan, N. T., Berrigan, C. S., Lopez, M.J.S. and Prasad, J.V.R., “Application of Linear Quadratic Estimation (LQE) to Harmonic Analysis of Rotorcraft Vibration,” Proceedings of the 72nd Annual Forum of the American Helicopter Society, West Palm Beach, Florida, May 17 – 19, 2016.

[8] Welch, G., Bishop, G., An Introduction to the Kalman Filter, TR 95-041, Department of Computer Science, University of North Carolina at Chapel Hill, July 24, 2006.

Copyright Statement